Accepted for publication in A&A on Jun 12$^{th}$ 2006

# Milne-Eddington inversions of the He I 10830 Å Stokes profiles: Influence of the Paschen-Back effect

C. Sasso, A. Lagg, and S. K. Solanki

Max-Planck-Institut für Sonnensystemforschung, Max-Planck-Str. 2, Katlenburg-Lindau, Germany



**ABSTRACT**

*Context.* The Paschen-Back effect influences the Zeeman sublevels of the He I multiplet at 10830 Å, leading to changes in strength and in position of the Zeeman components of these lines.

*Aims.* We illustrate the relevance of this effect using synthetic Stokes profiles of the He I 10830 Å multiplet lines and investigate its influence on the inversion of polarimetric data.

*Methods.* We invert data obtained with the Tenerife Infrared Polarimeter (TIP) at the German Vacuum Tower Telescope (VTT). We compare the results of inversions based on synthetic profiles calculated with and without the Paschen-Back effect being included.

*Results.* We find that when taking into account the incomplete Paschen-Back effect, on average 16% higher field strength values are obtained. We also show that this effect is not the main cause for the area asymmetry exhibited by many He I 10830 Stokes $V$-profiles. This points to the importance of velocity and magnetic field gradients over the formation height range of these lines.

**Key words.** Sun: chromosphere – Sun: magnetic fields – Sun: infrared

## 1. Introduction

Spectropolarimetry in the He I triplet at 10830 Å has become one of the key tools to determine the magnetic field vector in the upper chromosphere (Trujillo Bueno et al. 2002; Solanki et al. 2003). A reliable determination of the magnetic field in this region is important for obtaining a better understanding of the coronal heating mechanism and the coupling between the relatively cool photosphere and the hot corona.

The He I 10830 Å multiplet originates between the atomic levels $2^3S_1$ and $2^3P_{2,1,0}$. It comprises a 'blue' component at 10829.09 Å with $J_u = 0$ (Tr1), and two 'red' components at 10830.25 Å with $J_u = 1$ (Tr2) and at 10830.34 Å with $J_u = 2$ (Tr3) which are blended at solar chromospheric temperatures.

In previous papers (Solanki et al. 2003; Lagg et al. 2004) the analysis of the observed polarization in the He I 10830 Å multiplet for the determination of the magnetic field vector was carried out considering the linear Zeeman splitting (LZS) approximation. Socas-Navarro et al. (2004) demonstrated that the magnetic field vector from spectropolarimetry in the He I 10830 Å multiplet must be determined by considering the wavelength positions and the strengths of the Zeeman components in the incomplete Paschen-Back effect regime. They demonstrated that neglecting the Paschen-Back effect results in significant errors in the calculation of its polarization profiles. For example, Socas-Navarro et al. (2004) pointed out that the Paschen-Back effect produces a $\sim$ 25% reduction in the amplitude of the red component, which implies that the linear Zeeman effect theory underestimates the magnetic field strength. For a detailed presentation of the theory of the Zeeman and the Paschen-Back effects see, e.g., Landi Degl'Innocenti & Landolfi (2004).

Fig. 1 shows positions and strengths of the Zeeman components as a function of the magnetic field. The calculations are performed in two different ways, by using the LZS approximation or taking into account the incomplete Paschen-Back splitting (IPBS). The figure, produced using data kindly provided by Socas-Navarro et al., clearly shows that positions of the transitions are strongly influenced by the Paschen-Back effect, especially for magnetic field strengths above a few hundred Gauss. The relative strengths of the transitions also depend on the field strength. The shift in wavelength position and the asymmetric change of the strengths between the blue and the red Zeeman sublevels introduce asymmetries in the resulting Stokes $Q$, $U$ and $V$ profiles. In their paper Socas-Navarro et al. (2004) show that this asymmetry is strong enough to produce a measurable effect in the observations.

Here we present systematic tests of the influence of the Paschen-Back effect on parameters retrieved from Stokes profile observations of the He I triplet. We pay particular attention to the asymmetry of the Stokes $V$-profile. This parameter is often used to diagnose combined gradients of the velocity and the magnetic field along the line of sight (LOS), but the IPBS also introduces an asymmetry into the Stokes $V$-profiles. It is therefore of considerable interest to see if the asymmetry seen in many Stokes $V$-profiles of the He I 10830 Å triplet is due to the IPBS, or if this line parameter provides information on the structure of the upper solar chromosphere.

## 2. Methods and results

In order to calculate Zeeman components and strengths of the He I 10830 Å multiplet in the IPBS regime, we have improved the numerical code for the synthesis and inversion of Stokes profiles in a Milne-Eddington atmosphere (Lagg et al. 2004), by using the polynomial approximants as proposed by Socas-Navarro et al. (2005).

Fig. 2 compares the synthetic Stokes profiles of the He I 10830 Å multiplet for a 50 G and a 1000 G field, inclined by 30° with respect to the line of sight, obtained considering LZS only and

C. Sasso, e-mail: sasso@mps.mpg.de

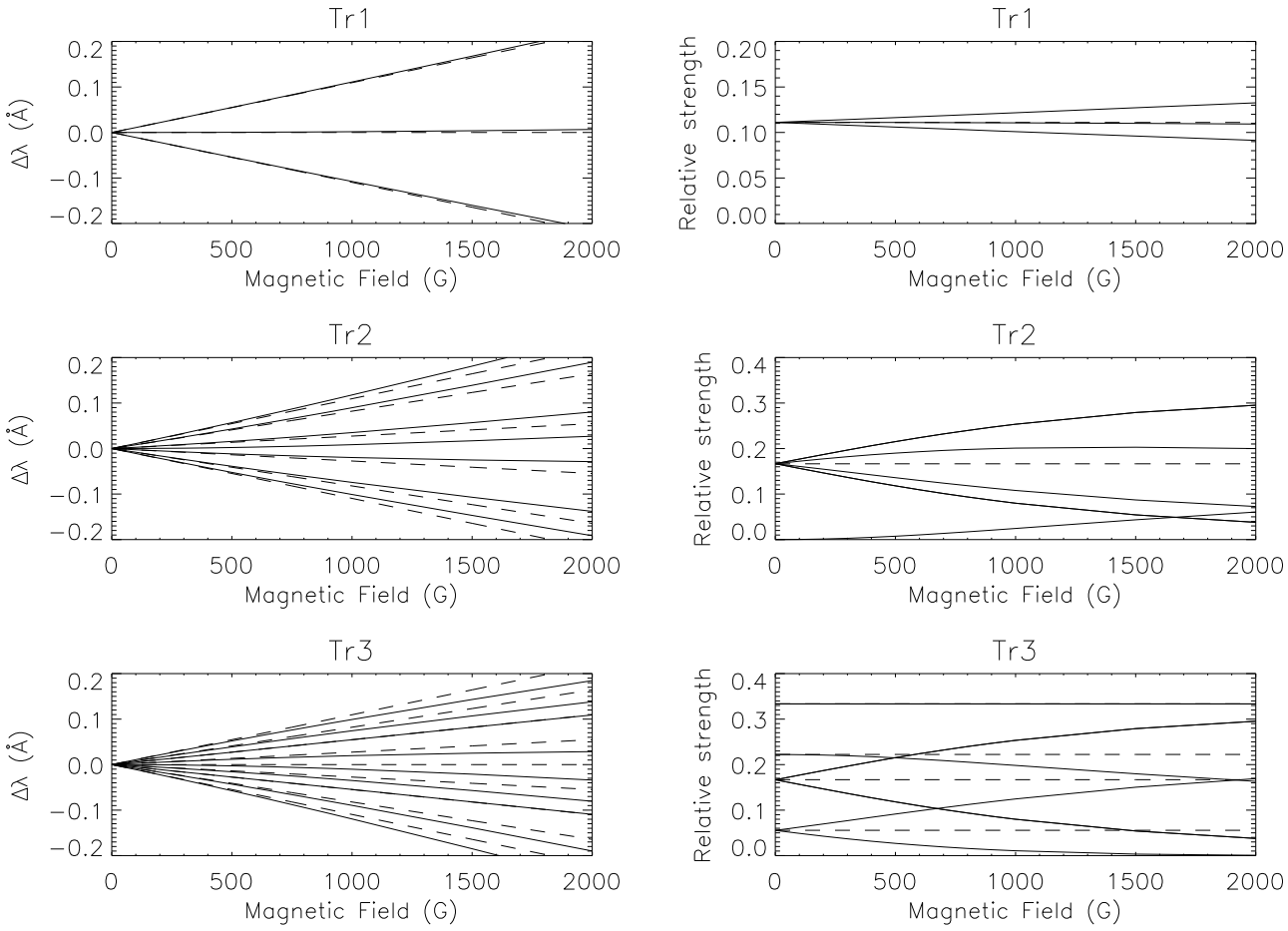


**Fig. 1.** Positions and strengths of the Zeeman components as a function of the magnetic field. The solid lines represent calculations considering the incomplete Paschen-Back splitting (IPBS), while the dashed lines represent those using the linear Zeeman splitting (LZS) approximation. In the IPBS case, the Zeeman components exhibit asymmetric displacement and strengths. This figure has been produced using data kindly provided by Socas-Navarro et al. (see Fig. 1 of Socas-Navarro et al. 2005).

including the IPBS. The difference between the profiles obtained when considering the IPBS (dotted line) or the LZS (dashed line) approximation, is clearly evident. For example, the $Q$ and $U$ profiles are symmetric and the $V$ profiles antisymmetric in the LZS case, while they are all asymmetric in the presence of IPBS. Moreover, if we compare the two panels we can see that the absolute difference between the profiles calculated using IPBS and LZS, increases with increasing magnetic field strength although the relative difference remains roughly the same (note the different vertical scales in the left and right parts of the figure). Note that in these tests we are using an effective Landé factor for each line of the multiplet for the LZS case, instead of the calculation of all Zeeman components separately, because this returns nearly identical results and a considerable gain in computation time (Lagg et al. 2004).

### 2.1. Inversion of synthetic profiles

In a next step we analysed the effect of the IPBS on synthetic Stokes profiles by estimating the error we make when retrieving the values of the physical parameters (such as the magnetic field vector, the LOS-velocity, etc.) by using LZS instead of IPBS. For this purpose we calculated synthetic profiles including IPBS, which are taken to represent an observation. We then inverted these IPBS profiles assuming LZS only. The difference between the original magnetic field and velocity values and the values retrieved from the LZS inversion are displayed in Fig. 3. We see, in both panels, a significant deviation of the retrieved values from the correct ones, indicated by the solid line at ordinate 0. More precisely, the error introduced by neglecting the IPBS increases with the strength of the magnetic field for both parameters and, for the LOS-velocity, it decreases with increasing inclination $\gamma$ of the magnetic field to the LOS. Neglecting IPBS gives artificial downflows of up to 350 m/s. On average the field strength is underestimated by 16% if IPBS is neglected, with the exact fraction lying in the range 14-18% depending on the magnetic field's inclination $\gamma$ and its azimuth, $\chi$.

The same analysis for the inclination and the azimuthal angle of the magnetic field shows that these two parameters are accurately retrieved by inversions even in the LZS approximation.

### 2.2. Inversion of observational data

We can now do a similar analysis using the observational data. We choose the observations of the emerging flux region NOAA 9451 located at 33°W, 22°S that were recorded with the Tenerife Infrared Polarimeter (Martínez Pillet et al. 1999) mounted behind the Echelle spectrograph on the Vacuum Tower Telescope at the Teide observatory on Tenerife. Fig. 4 displays Stokes $I$ maps for the observed region in the continuum and in the core of the He I line. This active region was previously studied assuming LZS (Solanki et al. 2003; Lagg et al. 2004). We

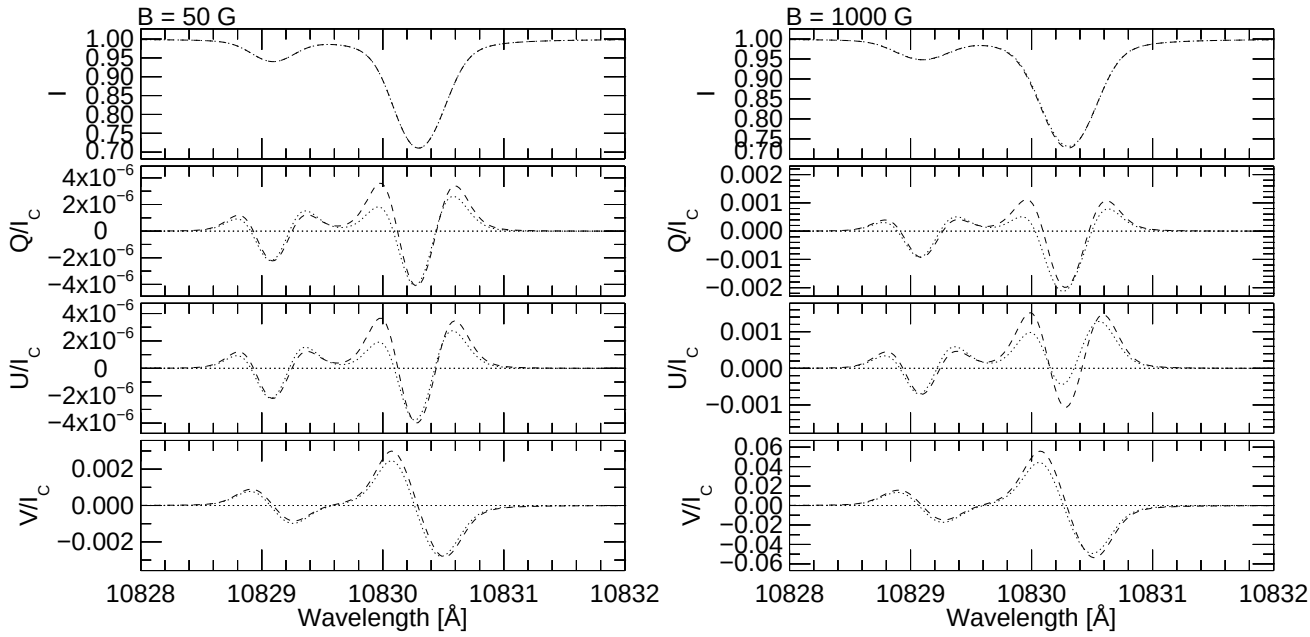


**Fig. 2.** Synthetic Stokes profiles of the He I 10830 Å triplet, assuming a 50 G (left) and a 1000 G (right) field, respectively, inclined by 30°with respect to the line of sight. The Milne-Eddington parameters we have used for this synthesis are: $\chi = 22.5°$, $v_{\rm LOS} = 0.0$ m/s, $a = 0.3$, $\Delta\lambda_{\rm D} = 0.2$ Å, $\eta_0 = 5.0$ and $\mu S_1 = 1.0$. (For the notation, see Lagg et al. 2004). The dotted profile is obtained by considering the IPBS, while the dashed one is obtained in the LZS approximation. The reference direction for Stokes $Q$ is along the $+y$-axis of the maps in Fig. 4.

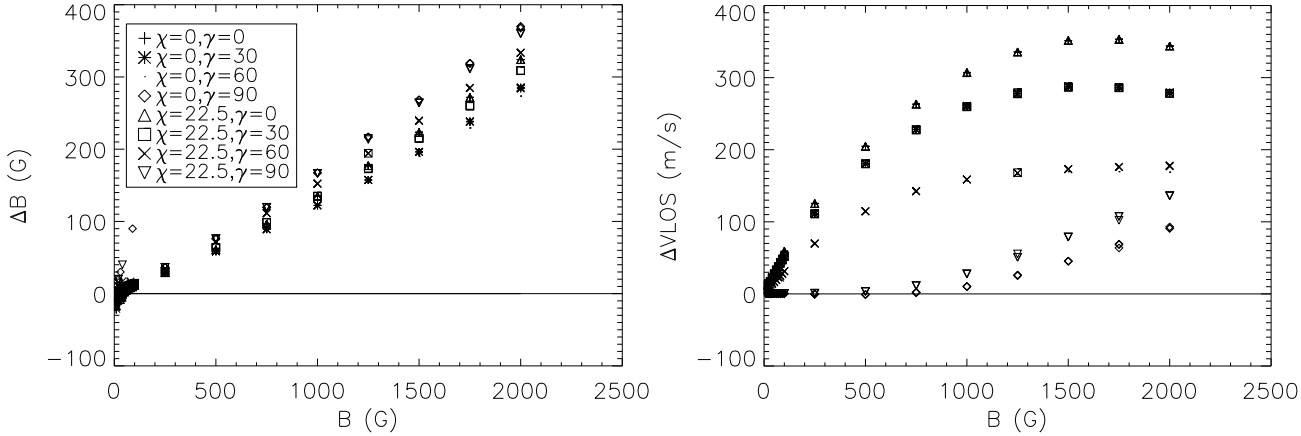


**Fig. 3.** On the left: Difference between the values of the magnetic field strength for a synthetic profile computed including IPBS and the ones obtained from the LZS inversion of this synthetic IPBS profile (ΔB), as a function of the magnetic field strength of the synthetic profile for different inclination ($\gamma$) and azimuthal angles ($\chi$) of the magnetic field vector (in degrees). On the right: The same for the LOS-velocity. The retrieved values for magnetic field (left) and LOS-velocity (right) deviate significantly from the correct values (horizontal solid line).

chose this particular observation for analysis partly because Socas-Navarro et al. (2004) suggest that some IPBS signatures described in their paper could be present in this observation referring, in particular, to profile asymmetries.

This data set is inverted twice, once in the LZS approximation and once including IPBS. All other particulars of the inversion remain unchanged. We consider the error in the retrieved value of the magnetic field strength if LZS is assumed when carrying out the inversions. Fig. 5 confirms the result shown in Fig. 3 that the retrieved magnetic field values are roughly 16% higher using the IPBS inversions. This result is also clearly displayed in the two maps of Fig 6. It implies that the field strengths at the chromospheric level in this region were underestimated by on average 16% by Solanki et al. (2003) and Lagg et al. (2004). We do not expect, however, that any of the main conclusions of these publications (or of Wiegelmann et al. 2005) are affected.

### 2.3. Stokes V asymmetry

In this section we evaluate the influence of the Paschen-Back effect on the Stokes $V$-profile relative area asymmetry defined as (Solanki & Stenflo 1984)

$$\delta\mathcal{A} = \frac{A_b - A_r}{A_b + A_r}, \tag{1}$$

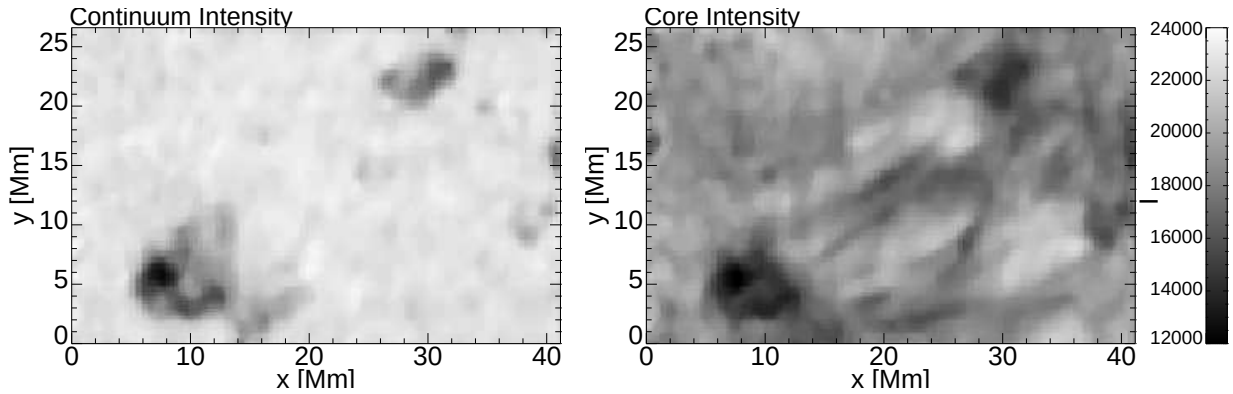


**Fig. 4.** Continuum (left) and He core (right) intensity maps of an emerging flux region (NOAA active region 9451, 33°W, 22°S)

where $A_b$ and $A_r$ (both positive) are, respectively, the areas of the blue and the red Stokes $V$-profile wings. The parameter $\delta\mathcal{A}$ is often used to provide information on the LOS gradient of the velocity and Bcos$\gamma$ in the height range of line formation (e.g. Solanki 1993). An alternative to this definition, which is more easily applicable to a whole multiplet (including complex-shaped profiles; Lagg et al. 2006), is the relative broad-band circular polarization

$$\delta V = \frac{\int_{-\infty}^{+\infty} V(\lambda) d\lambda}{\int_{-\infty}^{+\infty} |V(\lambda)| d\lambda}. \quad (2)$$

Socas-Navarro et al. (2004) investigated how the area asymmetry produced by the Paschen-Back effect varies with the magnetic field strength and pointed out that for a typical Doppler width of 105 mÅ, $|\delta V| \approx 0.11$ for $B < 1000$ G, which suggests that significantly larger observed values of $|\delta V|$ cannot be solely due to the effects of Paschen-Back effect splitting if the inferred B turns out to be smaller or similar to 1000 G.

In Fig. 7 (left panel) we plot the absolute value of the relative broad-band circular polarization ($|\delta V|$) of the best-fit IPBS $V$-profiles to the observed profiles as a function of the magnetic field strength for different ranges of the values of the e-folding width of the lines. The $\delta V$ is calculated over the whole wavelength range of the He multiplet. The $|\delta V|$ of the best-fit synthetic IPBS $V$-profiles is nearly independent of B, but is a strong function of the width of the lines, as indicated by different symbols. This behaviour is displayed more clearly in the right panel of Fig. 7 where we plot $|\delta V|$ as a function of the width of the lines. We expect that the $|\delta V|$ of the observed profiles should exhibit a similar dependence, if $|\delta V|$ solely results from the IPBS. The $|\delta V|$ of the observed profiles (see dots in Fig. 8, left panel) clearly shows no such dependence. In order to test if noise is the reason for the lack of this dependence we add random noise to the synthetic IPBS $V$-profile of the same order as the one we have in the observational data. We restrict our analysis to synthetic profiles with a maximum $V$-signal at least three times higher than the noise level and to the corresponding observed profiles. The $|\delta V|$ of synthetic, noisy IPBS $V$-profiles (represented by crosses in the left panel of Fig. 8) retains the dependence on the width of the lines. Fig. 8 (left) shows that the observed $|\delta V|$ values can be up to 4 times as large as those of the synthetic profiles. Values of the observed $|\delta V| \geq 0.2$ cannot be explained by IPBS or noise. The difference between the two sets of $|\delta V|$ values is displayed more markedly in the right panel of Fig. 8, where the values are grouped into bins containing the same number of points. For each bin the mean value is displayed in the x- and y-coordinates. Moreover, the difference between the $\delta V$ values

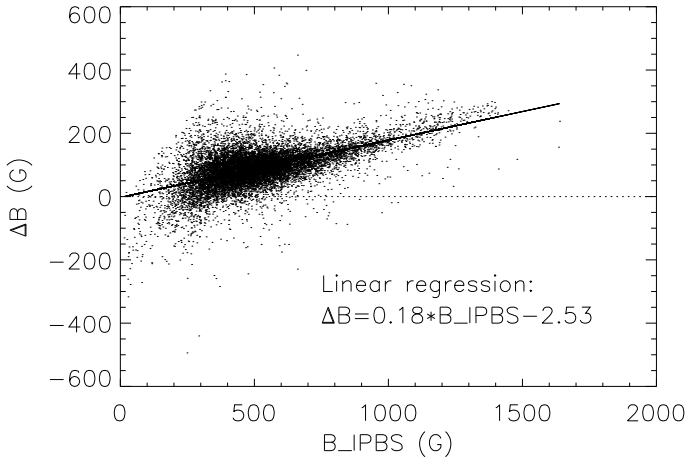


**Fig. 5.** Influence of IPBS on the retrieval of the magnetic field strength for NOAA 9451. Difference in field strength, ΔB, deduced from inversions including the IPBS, $B_{IPBS}$, and those without it, versus $B_{IPBS}$. The solid line represents a linear regression. The larger scatter present in the figure for $B_{IPBS} \leq 800$ G is due to the noise that affects the observation.

of the synthetic IPBS $V$-profiles and of the observed $V$-profiles is even larger than suggested by Fig. 8 because, for 54% of the profiles, they have opposite sign. Consequently, another mechanism must be acting to produce at least the larger values of the asymmetry. The most obvious one is the combination of velocity and magnetic-field gradients (see Solanki 1993, for a review). Support for this mechanism comes from the fact that the observed $\delta V$ is larger for narrow lines, for which smaller velocity and magnetic-field gradients are required to produce a large $\delta V$ (Grossmann-Doerth et al. 1989).

## 3. Conclusions

We analysed the influence of the Paschen-Back effect on the Stokes profiles of the He I 10830 Å multiplet lines, estimating its relevance using synthetic profiles and investigating its influence on the inversion of a spectropolarimetric scan of an emerging active region.

Our results support the conclusion of Socas-Navarro et al. (2004) that IPBS should be taken into account when modeling the polarization profiles of the He I 10830 multiplet. For example, we found that by including the incomplete Paschen-Back effect into our inversion code, on average 16% higher field strength values are retrieved from inversions, while other atmospheric pa-

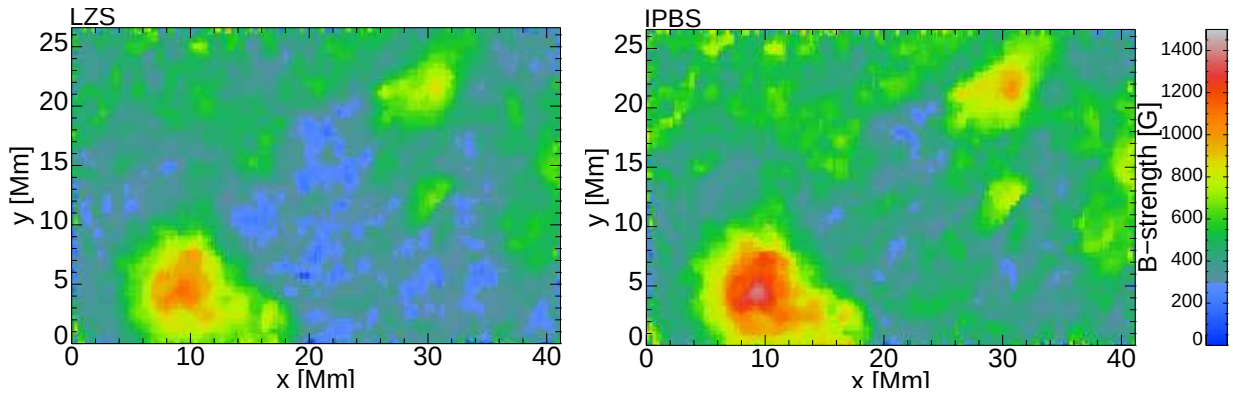


**Fig. 6.** Maps of magnetic field strength of the active region shown in Fig. 4. Left frame: result of an inversion assuming LZS; right frame: the same, but with IPBS. Note that both images have the same colour scale.

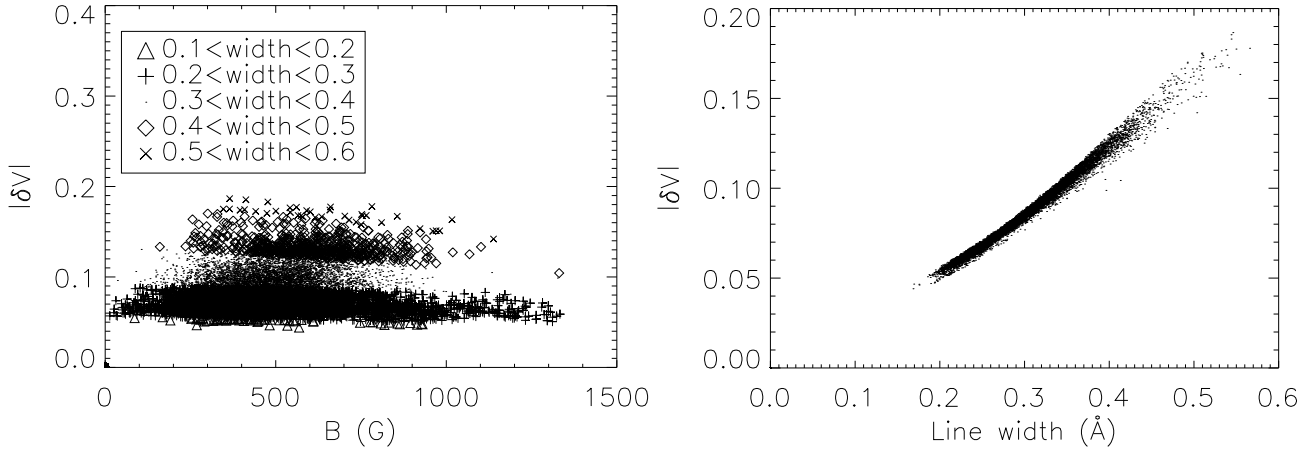


**Fig. 7.** Left: Absolute value of the relative broad-band circular polarization ($|\delta V|$) of synthetic IPBS $V$-profiles as a function of the magnetic field strength. The symbols distinguish between different ranges of the e-folding width of the lines. Right: $|\delta V|$ as a function of the width of the lines.

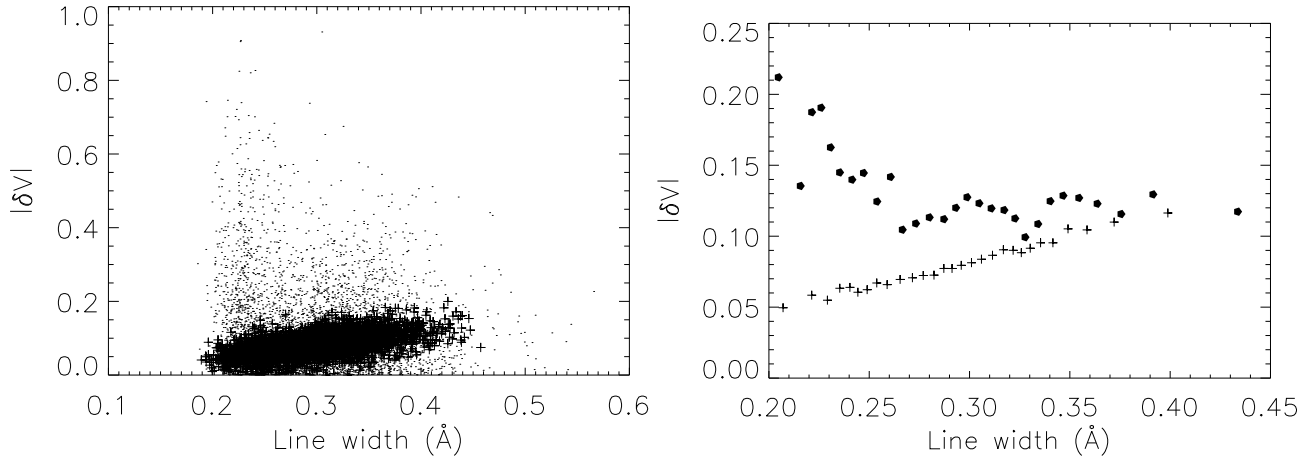


**Fig. 8.** Left: Absolute value of the area asymmetry of the fitted, synthetic IPBS $V$-profiles (crosses) to which we have added random noise and of the observed $V$-profiles (dots) as a function of the line width. Right: The same, but here the values are averaged over bins containing the same number of points.

rameters are affected less significantly.

We also showed that the Paschen-Back effect is not the main cause for the area asymmetry exhibited by the many He I 10830 Stokes profiles that showed a line width smaller than ~ 0.30 Å in Lagg et al.'s (2004) emerging flux region observation. The spatial points corresponding to such Stokes $V$-profiles are those for which the inferred value of the magnetic field strength is lower than ~ 1.1 kG when IPBS is taken into account. The fact that the area asymmetry of the observed $V$-profiles is considerably stronger than of the synthetic $V$-profiles indicates that some other effect drives the area asymmetry more strongly than the

Paschen-Back effect. The main candidates are LOS-gradients of the magnetic field vector and the velocity.

*Acknowledgements.* We would like to thank Hector Socas-Navarro and Javier Trujillo Bueno for helpful discussions regarding the Paschen-Back effect and for providing material from their publications. We also thank Joachim Woch, Norbert Krupp and Manolo Collados for their help during the observing run. This work was supported by the program "Acciones Integrades Hispano-Alemanas" of the German Academic Exchange Service (DAAD project number D/04/39952).

## References

Grossmann-Doerth, U., Schüssler, M., & Solanki, S. K. 1989, A&A, 221, 338
Lagg, A., Woch, J., Krupp, N., & Solanki, S. K. 2004, A&A, 414, 1109
Lagg, A., Woch, J., Solanki, S. K., & Krupp, N. 2006, A&A submitted
Landi Degl'Innocenti, E., & Landolfi, M. 2004, Polarization in Spectral Lines (Kluwer Academic Publishers)
Martínez Pillet, V., Collados, M., Sánchez Almeida, J. et al. 1999, in High Resolution Solar Physics: Theory, Observations, and Techniques (Astronomical Society of the Pacific), ASP Conf. Ser., 183, 264
Socas-Navarro, H., Trujillo Bueno, J., & Landi Degl'Innocenti, E. 2004, ApJ, 612, 1180
Socas-Navarro, H., Trujillo Bueno, J., & Landi Degl'Innocenti, E. 2005, ApJS, 160, 312
Solanki, S. K., & Stenflo, J. O. 1984, A&A, 140, 185
Solanki, S. K. 1993, Space Sci. Rev., 63, 1
Solanki, S. K., Lagg, A., Woch, J., Krupp, N., & Collados, M. 2003, Nature, 425
Trujillo Bueno, J., Landi Degl'Innocenti, E., Collados, M., Merenda, L., & Manso Sainz, R. 2002, Nature, 415, 403
Wiegelmann, T., Lagg, A., Solanki, S. K., Inhester, B., Woch, J. 2005, A&A, 433, 701